Graph Embedding Using Frequency Filtering

Hoda Bahonar, Abdolreza Mirzaei, Saeed Sadri, Richard C. Wilson, *Senior Member, IEEE*

Abstract—The target of graph embedding is to embed graphs in vector space such that the embedded feature vectors follow the differences and similarities of the source graphs. In this paper, a novel method named Frequency Filtering Embedding (FFE) is proposed which uses graph Fourier transform and Frequency filtering as a graph Fourier domain operator for graph feature extraction. Frequency filtering amplifies or attenuates selected frequencies using appropriate filter functions. Here, heat, anti-heat, part-sine and identity filter sets are proposed as the filter functions. A generalized version of FFE named GeFFE is also proposed by defining pseudo-Fourier operators. This method can be considered as a general framework for formulating some previously defined invariants in other works by choosing a suitable filter bank and defining suitable pseudo-Fourier operators. This flexibility empowers GeFFE to adapt itself to the properties of each graph dataset unlike the previous spectral embedding methods and leads to superior classification accuracy relative to the others. Utilizing the proposed part-sine filter set which its members filter different parts of the spectrum in turn improves the classification accuracy of GeFFE method. Additionally, GeFFE resolves the cospectrality problem entirely in tested datasets.

Index Terms—Spectral graph embedding, graph Fourier transform, heat kernel, frequency filtering, graph classification

1 Introduction

The key issue in pattern recognition is the formal definition of pattern space, which is able to represent all discriminative information among different objects. The classical statistical pattern recognition follows this goal using vectors as the object representation formalism. There exists a wide range of well-defined operators and well-developed efficient algorithms in this approach [1], [2]. Nevertheless, the nature of patterns in some cases such as bioinformatics and chemistry [3], document analysis [4], network traffic control [5] and images classification [6] are not only dependent on features, but also structural relations between them. In these situations, graphs are versatile alternatives to feature vectors. However, graphs are not intrinsically vectorial, which leads to increased complexity of many algorithms in the graph domain. For example, comparison of two vectors is done in linear time, while comparison of two graphs (graph isomorphism) has exponential complexity. This behavior is observed because, unlike the samples of a vector, there is no standard ordering for the nodes and edges in a graph. Similarly, it is non-trivial to define some basic operators required for many algorithms such as sum and product in the context of graphs. So only a few pattern recognition algorithms which are usually based on distance and its derivatives have direct counterparts in the graph domain [7], [8], [9]. The graph algorithms of this type come from a classical period of graph based pattern recognition [8]. In the modern period, two major approaches have been followed for making use of the powerful existing algorithms of statistical pattern recognition, namely kernel-based methods and embedding methods. Kernel-based methods replace dot product with a graph kernel in algorithms which are formulated in terms of dot products [10], [11], [12].

Graph embedding methods extract structural features from graph and put them together in a vector format to make use of algorithms which process and analyze feature vectors directly [13], [14]. So graph embedding offers an easy solution for machine learning problems using the power of graphs as symbolic data structures and computational advantage of feature vectors. Two main requirements of embedded feature vectors are that they are invariant and informative. Being invariant means that the embedded vectors should be the same for every selected node/edge ordering. These vectors should be informative as well, i.e. they should contain enough discriminative features such that similar structures are close together and different structures are far away from each other in the embedding space [14].

Employing graph spectra is a natural way for extracting invariants in an acceptable time. There are a variety of methods in this area [6], [14], [15], [16], [17], [18]. The question is if the feature vectors extracted by these methods are informative enough to have good performance in different applications. The discriminative structures vary from one application to another. In some applications, the features based on small scale connectivity perform better, while the large-scale structures are better candidates for others [19]. The cycles, paths, and loops have different importance in recognizing the patterns of different graph sets [17]. So for the embedding method being universal, it should be flexible enough to represent any type of graph similarities. This flexibility is not observed in previous embedding methods as their properties are the same regardless of the application in hand.

A possible solution for lowering this limitation is to exploit different spectral methods to form a high dimensional feature vector and train the most informative features to adapt to the structural properties of the graph set as proposed in [20]. But the power of this mixed strategy is limited to the power of the methods used, and redundant features may make it more difficult to find the important discriminative

- *H. Bahonar, A. Mirzaei and S. Sadri are with the Department of Electrical and Computer Engineering, Isfahan University of Technology, Isfahan 84156-83111, Iran.*
  E-mail: h.bahonar@ec.iut.ac.ir, mirzaei@cc.iut.ac.ir, sadri@cc.iut.ac.ir
- *R. C. Wilson is with Department of Computer Science, University of York, UK.*
  E-mail: Richard.Wilson@york.ac.uk

features.
Fourier analysis provides better understanding of the signal by transferring it to another domain [21]. This behavior is very useful while important features are not easily discoverable in the original domain [22], [23], [24]. For example, one way for edge detection is to locally search within the image to find a sharp change in the brightness of the pixels. However this operation needs scanning all the pixels to compare the brightness of them and their neighbors. Fourier analysis makes this approach easier by filtering the high frequencies. In other words, edge features of original domain spread all over the image, but when these features are transformed into the Fourier domain, their information is limited to a narrow range of frequency values. More generally, Fourier analysis creates a kind of scale-space representation, with small-scale features represented in the high frequencies and large-scale structure in the low frequencies.
Similarly, the key information in graphs appears at different scales (i.e. frequencies) in different applications. For example when predicting the domain of a protein graph, the large-scale organization of the protein is likely to be important. On the other hand, in protein interaction networks, we might expect the detailed interactions to be more important. This is also supported by our previous work on diffusion wavelets [19]. Therein, Fourier analysis is likely to be a successful strategy for discovering the features on different scales of the graph structure. There is a sound definition for graph Fourier transform in the context of graph signal processing [25] which provides the notion of frequency in the Fourier domain. Image signal denoising [26], analysis of brain imaging [27], video compression [28] and network traffic analysis [29] are some applications of this context. Indeed, graph signal processing has emerged for better signal understanding using the relations (represented by edges) of the signal samples (represented by nodes). Of course the application of the graph signal processing is limited to analysis, processing and making decision about the nodes of just one graph.
In the context of graph embedding, the samples under study are graphs, not the graph nodes. So discovering the most informative features for this context needs separate investigation. Our goal in this paper is to utilize ideas from the graph Fourier transform to generate a general set of graph features which represent a kind of scale space for the graphs. We can then learn which of these features are important in particular applications. The contributions of this paper can be outlined as follows:

1) The main contribution is to use graph signal processing methods in order to embed graphs in vector space. The representation of the graph in Fourier domain and its related operators are chosen for making invariants as a first step. Then frequency filtering is suggested, as a Fourier domain operator, to make the invariant more informative.
2) Frequency Filtering Embedding (FFE) method is proposed whose vectors are the graph responses to some pre-defined filter functions. Heat, Anti-heat, part-sine, and identity filter sets are proposed which have different properties in discovering the latent features in different frequencies.
3) The pseudo-Fourier operators are proposed as the generalization of Fourier transform. Based on these operators and frequency filtering operator, Generalized Frequency Filtering Embedding (GeFFE) is proposed. This embedding method can be regarded as a general framework for some previously introduced invariants such as Laplacian spectrum and eigen-mode.
4) It is shown that the flexibility of using different filter functions and different pseudo-Fourier operators, enables GeFFE to adopt itself to the properties of different datasets.
5) Using eigenvalues and eigenvectors at the same time enables GeFFE to resolve cospectrality problem in tested datasets.
6) GeFFE can be regarded as a general-purpose embedding method, because its feature vectors are trained to reflect the different meanings of similarity and dissimilarity in different datasets.

After reviewing the literature of graph embedding in Section 1.1, some preliminaries for better understanding the paper issues are presented in Section 1.2. The different aspects of the proposed methods are declared in Section 2. The experimental results are illustrated in Section 3 and finally in Section 4 the conclusion remarks and the future trend are clarified.

1.1 Related Work

Graph embedding methods can be divided into three groups: probing-based, dissimilarity-based and spectral methods. A straightforward approach for embedding graphs is probing the graph to enumerate the occurrence frequencies of special substructures [30]. This approach depends on subgraph isomorphism which is an NP-complete problem. So in recent years, probing-based methods tend to utilize the information contained in smaller substructures, usually limited to one node/edge or two adjacent nodes/edges [31], [32]. For example, Luqman et al. [31] proposed to use subgraph homogeneity features, composed of two histograms. The first shows the label homogeneity of nodes on both ends of the edges and the second shows the label homogeneity of edges adjacent to the nodes. Taking just these local label information into account decreases the computational complexity of probing-based methods, but discarding more global substructures increases the possibility of extracting the same feature vector for completely different graphs substantially.
The more accurate approach which is based on idea presented in [33] is dissimilarity-based graph embedding [34], [35], [36], [37]. Riesen and Bunke [38] embedded the graphs into vector space by their dissimilarity values to some selected prototype graphs. The graph edit distance which is used as the dissimilarity measure in this method is defined as the minimum cost for converting one graph to another by edit operations. Graph edit distance makes dissimilarity-based graph embedding method flexible enough to apply on different graph domains including unlabeled as well as categorical/numerical labeled graphs. But due to high complexity of graph edit distance computation, the dissimilarity-based method is just applicable on small graphs [39].
Spectral graph embedding methods extract the graph fea-

tures using components, eigenvalues (spectrum) and eigenvectors of graph representation matrices. The spectral methods have intermediate computational complexity and intermediate accuracy. These methods rely on extensive researches in the field of spectral graph theory [40], so it is not surprising that there are diverse ongoing methods in this group of graph embedding methods. For example, Luo et al. [6] derived the unary and binary features from the eigen-modes (eigenvalues and eigenvectors) of graph adjacency matrix A. The unary features are computed from each eigen-mode independently, such as the vector of largest eigenvalues. The binary features are computed from binary interactions of eigen-modes. For example, the value in row i and column j of inter-mode adjacency matrix is the result of inner product of ith eigenvector, the adjacency matrix, and jth eigenvector. In hypergraphs domain, Ren et al. [15] utilized some smallest eigenvalues of the Laplacian matrix L which is obtained from the adjacency matrix and conveys better information about nodes connectivity relative to adjacency matrix. In another work [16], they used Perron-Frobenius operator which contains information about edge interactions. In order to extract permutation invariant features from this operator, they used selected polynomial coefficients of Ihara function defined on Perron-Frobenius operator and formed the Ihara coefficients vector. Aziz et al. [17] introduce backtrackless walks as a related concept to Ihara coefficients. They embedded graphs by the number of backtrackless paths of different lengths which can be computed from the powers of Perron-Frobenius operator. Ihara coefficients and backtrackless walks are less prone to cospectrality (i.e. the problem of having same vector for different graphs) relative to the Laplacian spectrum, because they use more structural information by getting Perron-Frobenius operator involved, but computing this operator is computationally expensive.

Another method for cospectrality reduction is getting eigenvectors elements involved in embedding. Wilson et al. [14] tried to take full advantage of the information included in eigenvectors by getting help from symmetric polynomials. The output of these functions does not depend on the order of their inputs. Their elementary symmetric polynomials which are utilized for making invariant from eigenvectors entities are defined as follows:

$$\begin{aligned}
&S_1(\phi_{i1},\phi_{i2},\ldots,\phi_{iN}) = \sum_{j=1}^{N}\phi_{ij}\\
&S_2(\phi_{i1},\phi_{i2},\ldots,\phi_{iN}) = \sum_{j=1}^{N}\sum_{k=j+1}^{N}\phi_{ij}\phi_{ik}\\
&\vdots\\
&S_r(\phi_{i1},\phi_{i2},\ldots,\phi_{iN}) = \sum_{j_1<j_2<\cdots<j_r}\phi_{ij_1}\phi_{ij_2}\ldots\phi_{ij_r}\\
&\vdots\\
&S_N(\phi_{i1},\phi_{i2},\ldots,\phi_{iN}) = \prod_{j=1}^{N}\phi_{ij}.
\end{aligned} \tag{1}$$

where $\phi_i = (\phi_{i1},\ldots,\phi_{iN})$ is the ith eigenvector. Applying these N functions on the elements of N eigenvectors results in N^2 values which are inserted in graph feature vector. They showed that the eigenvector elements can be obtained from these N^2 values of symmetric polynomials. So these values contain all information of eigenvectors and they are node permutation invariant. But the high dimensionality of the resultant vector has a destructive impact on accuracy of embedded vectors in applications.

The heat kernel has proved an effective concept in spectral graph analysis [18]. This concept provides a metric for evaluating the amount of information flow from one node to another. The heat kernel amount from node x to node y in time t is computed as:

$$K_t(x,y) = \textstyle\sum_{l=1}^{N} e^{-\lambda_l t}\phi_l(x)\phi_l(y), \tag{2}$$

where (λ_l,ϕ_l) are lth eigenvalue and eigenvector of Laplacian matrix. Apparently, the heat kernel describes the relation between the nodes of one graph, as it is employed in studying geometric [41] and hierarchical [42] characteristics of graphs and graph node signature [42], [43]. For example, Sun et al. [42] proposed a signature for a graph node as the amount of transmitted heat from that node to itself during some pre-specified time steps and called it Heat Kernel Signature (HKS). There are some attempts to extract invariants from the heat kernel to utilize it in graph embedding. Wilson [44] proposed to use histogram of node HKSs or long vector of their sorted values as the graph feature vector. Xiao et al. [45] proposed embedding graphs using three invariants of heat kernel including heat kernel trace, zeta function derivative, and power series expansion coefficients of heat content. We propose a systematic approach to transfer heat kernel to graph embedding scope. This approach can be regarded as a general framework which produces some other beneficial concepts rather than heat kernel as special cases by a notion of parameterization.

1.2 Preliminaries

An unlabeled graph G is an ordered set $G = (V,E)$, where V is the node set and $E \subseteq V \times V$ is the edge set of the ordered pairs of nodes. The graph edit distance between graphs G_1 and G_2 is defined as the minimum cost of converting G_1 to G_2 by consecutive edit operations. Edit operations are defined according to the graph domain and edit operation costs are assigned to each edit operation based on application. For example, in unlabeled graphs domain, edit operations can be defined as {node insertion, node deletion, edge insertion, edge deletion} and the cost can be the same for all edit operations. The edit distance is considered to be the 'gold-standard' comparison between two graphs, but is NP-hard to compute in general. A good graph embedding should match the edit distance as closely as possible. Two common graph representation matrices for extracting structural information from graphs are adjacency and Laplacian matrices. The adjacency matrix A is a $|V|\times|V|$ matrix which is defined as:

$$A(i,j) = \begin{cases} 1 & \text{if } (i,j)\in E \\ 0 & \text{otherwise.} \end{cases} \tag{3}$$

The graph Laplacian matrix is given by $L = D - A$, where D is the diagonal $|V|\times|V|$ matrix of node degrees which is defined to be:

$$D(i,j) = \begin{cases} \sum_{(i,k)\in E} A(i,k) & \text{if } i = j \\ 0 & \text{otherwise.} \end{cases} \tag{4}$$

(λ_l, ϕ_l) is lth graph eigen-mode which is composed of lth eigenvalue of the selected representation matrix and its related eigenvector, respectively. The selected representation matrix in this paper is Laplacian matrix.

A graph signal is a function $g : V \rightarrow \mathbb{R}$, applied to the graph nodes and results in the vector $g \in \mathbb{R}^N$, where $g(m)$ is the value assigned to mth graph node and N is the number of graph nodes. An unlabeled graph can be regarded as a constant graph signal with $g(m) = 1$, for all nodes m. In the discussions of this paper, the two concepts of graph and the representative graph signal can be used interchangeably. So, from now on we use G for referring to both graph and its graph signal, i.e. $G(x)$ is a graph signal on graph G . Regarding the notion of frequency of the Laplacian eigenvalues [25], the graph Fourier transform and the inverse graph Fourier transform are defined respectively to be:

$$\hat{G}(\lambda_l) = \langle G, \phi_l \rangle = \sum_{x=1}^{N} G(x)\phi_l^*(x), \tag{5}$$

$$G(x) = \sum_{l=1}^{N} \hat{G}(\lambda_l)\phi_l(x), \tag{6}$$

where G is a graph signal, $\langle ., . \rangle$ is the inner product and * is the conjugate operator. The graph Fourier transform is therefore defined on the domain of eigenmodes of the graph and graph eigenvalues play the role of frequencies in this definition. In other words, $\hat{G}$ is the function of the eigenmode whose λ_l is representative. Frequency filtering is an operator in Fourier domain which amplifies or attenuates some frequencies and is defined as:

$$\hat{G}_{out}(\lambda_l) = \hat{G}_{in}(\lambda_l)\hat{F}(\lambda_l), \tag{7}$$

where $\hat{F}(.)$ is the filter function whose inputs are eigenvalues.

There is a relation between heat kernel and Fourier transform established in [25] which is as follows. Assume G as the initial heat on the graph nodes. The heat amount on each node x at time t, $H_tG(x)$, can be found by:

$$H_tG(x) = \sum_{y=1}^{N} K_t(x, y)G(y), \tag{8}$$

where $K_t(x, y)$ (from eq. 2) is the transmitted heat from node x to node y at time t. $H_tG(x)$ is total transmitted heat from node x to all other nodes in time t. Inserting eq. 2 into eq. 8 and rearranging the $\sum$ operators, we have:

$$H_tG(x) = \sum_{l=1}^{N} \sum_{y=1}^{N} G(y)e^{-\lambda_l t}\phi_l(y)\phi_l(x). \tag{9}$$

Using eq. 6:

$$H_tG(x) = \sum_{l=1}^{N} \widehat{H_tG}(\lambda_l)\phi_l(x). \tag{10}$$

Comparing 9 and 10, it can be concluded that:

$$\widehat{H_tG}(\lambda_l) = \sum_{y=1}^{N} e^{-\lambda_l t}G(y)\phi_l(y) = e^{-\lambda_l t}\hat{G}(\lambda_l). \tag{11}$$

Comparing eq. 11 and eq. 7, H_tG is the result of frequency filtering on G by filter function $\hat{H}_t(\lambda_l) = e^{-\lambda_l t}$.

2 Proposed methods

As it is apparent in graph signal definition, there is an implicit pre-specified node ordering in a graph signal. The graph Fourier transform (eq. 5) provides a mapping from node order dependant signal into a node order independent one based on the graph structure:

$$\begin{aligned}&[G(v_1), G(v_2), \ldots, G(v_N)]\\ &\xrightarrow{\text{graph fourier transform}} [\hat{G}(\lambda_1), \hat{G}(\lambda_2), \ldots, \hat{G}(\lambda_N)].\end{aligned} \tag{12}$$

At first glance the graph representation in Fourier domain can be used as an invariant in graph embedding. The power of this embedding depends on the graph signals of the application. Here we focus on using frequency filtering to obtain more discriminative and useful graph features for particular applications.

2.1 Frequency Filtering Embedding

As it is mentioned in Section 1.1, the heat kernel has proved useful in exploring graph structure. Eq. 8 provides a mechanism to have a numerical measure for impact power of a kernel on each node. This numerical measure for heat kernel, H_tG, has been used in signal domain previously but not in Fourier domain. Considering eq. 11 which shows that H_tG is the result of applying filter function $e^{-\lambda_l t}$ to G, we propose to use $e^{-\lambda_l t}$ for some values of t as well as some other filter functions for graph embedding in vector space. So, Frequency Filtering Embedding method is proposed as follows:

Definition 1. *Frequency Filtering Embedding (FFE):* Let $\mathcal{F} = \{F_1, F_2, \ldots, F_r\}$ be the filter bank, where $F_i : \mathbb{R} \rightarrow \mathbb{R}$ is a filter function. The frequency filtering embedding $\gamma_{\mathcal{F}}$ is defined as:

$$\begin{aligned}&\gamma_{\mathcal{F}} : \mathcal{G} \rightarrow \mathbb{R}^{m \times r}\\ &\gamma_{\mathcal{F}}(G) = [\mathbf{f}_1(G)^T, \mathbf{f}_2(G)^T, \ldots \mathbf{f}_r(G)^T],\end{aligned} \tag{13}$$

where $\mathcal{G}$ is the graph domain, m is the number of selected eigen-modes and $\mathbf{f}_k(G) = [F_k(\lambda_j)\hat{G}(\lambda_j), j = 1, \ldots, m]$ is the response of graph G to the filter F_k. where $\hat{G}$ is the Fourier transform of graph G. Here $m = N$, because utilizing all the eigen-modes is of interest. □

2.2 The proposed filter function sets

The heat filter set members for $1 \leq t \leq 6$ are shown in Fig. 1(a). As it was mentioned before, their equation is:

$$H_t(\lambda_l) = e^{-t\lambda_l}. \tag{14}$$

These filters amplify the low frequencies and their values decay rapidly by increasing the magnitude of the eigenvalues. This rapidity is greater for the greater values of t. So the frequency filtering by each of these functions puts its emphasis on the structures whose effect is exposed in the low frequencies. The heat filter function set is useful where noise affects mostly on the small scale structures like individual edges, and this noise can be removed significantly by removing the high frequencies, the most important features occur in the large scale interactions (low frequencies), and the effect of the small scale sub-structures can be safely removed. Although the usefulness of the heat functions for describing the between node relations of one graph is confirmed by several previous researches as mentioned in Section 1.1, the experiments confirm that other filter functions which put their emphasis on the other portions of the spectrum may convey more information regarding to

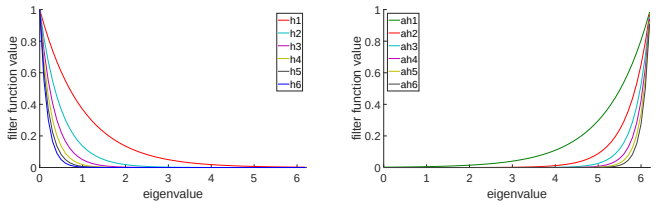

(a) heat filters

(b) anti-heat filters

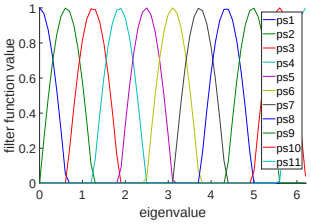

(c) part-sine filters

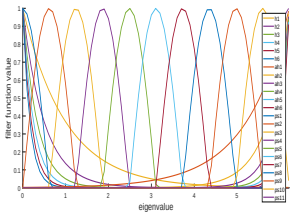

(d) all filters except X

Fig. 1: The proposed filter function sets.

the application in hand. Here utilizing three other filter sets are proposed. The anti-heat filter set is the second used filter set, shown in Fig 1(b). These filters are computed with the following equation:

$$AH_t(\lambda_l) = e^{-t(R-\lambda_l)}, \tag{15}$$

where R is the end point of the eigenvalues range. It can be seen that unlike the heat filter functions, in these filters, the emphasis is on the high frequencies. Unlike the heat filter set, the anti-heat filter functions are useful where the important features reside in the small interactions, so the high frequencies can not be removed. The low frequencies can be disregarded, because they possess redundant or unrelated features. The third filter set, shown in Fig. 1(c) is the part-sine filter set whose every member emphasize on a special portion of the spectrum and is calculated as follows:

$$PS_{r,\rho}(\lambda_l) = \begin{cases} sin\frac{\pi}{2\rho}(\lambda_l - \rho(r-2)) & \text{if } \rho(r-2) \leq \lambda_l \leq \rho r \\ 0 & \text{otherwise,} \end{cases} \tag{16}$$

where ρ is the number of sub-ranges the part-sine functions defined on and r is their sequence number. For the situations that the most effective frequencies are unknown or the important information spread over the entire frequency domain, the part-sine filters are good candidates. Dividing the spectrum into different sub-ranges, separates the effects of the features of different scales. Considering the entire spectrum equips us with all the features, including effective, non-effective and noisy features. The undesired features can be removed in subsequent steps. Fig 1d displays the mentioned filters together for comparison. The last filter is $X(\lambda_l) = \lambda_l$. This filter is appended to the filter set for generalizing the proposed method, as it will be shown in Section 2.4.

2.3 Pseudo-Fourier operators

FFE has the potential to be a general-purpose embedding method, because it makes use of both eigenvalues and eigenvectors simultaneously. The effect of the eigenvalues can be adjusted in FFE by changing the filter function. Another flexibility which is needed for generalizing FFE is the feasibility of defining different combinations of eigenvector elements. This feasibility is not provided by FFE, because it represents a linear transform of the original representation. Despite being invariant, the graph Fourier transform does not always provide so much information about the graph structure. For a constant graph signal, the Fourier transform is given by $\hat{G}(\lambda_l) = \sum_{x=1}^{N} \phi_l(x)$ which is equal to $S_1(\phi_l)$ of symmetric polynomials (eq. 2). Because of these two reasons, providing some new operators rather than Fourier transform using some different combination strategies on the elements of eigenvectors can be helpful. We call these operators as pseudo-Fourier operators (PFOs). A PFO should preserve these conditions:

1) It should possess the notion of frequency like in the Fourier transform, i.e. it should preserve the property that by moving towards the greater eigenvalues, the number of changes in the values of the eigenvector elements decreases or increases monotonically.
2) It should be able to formulate the methods which use just the eigenvalues as the special cases. For instance, the Laplacian spectrum is a relatively strong method which FFE cannot formulate.
3) It should promote the capability of pattern recognition of graphs relative to the mere use of Fourier transform in FFE. Additionally, it should formulate FFE as the special case.

The PFOs are motivated by a number of factors. Firstly, PFOs are directly related to the symmetric polynomials [14], introduced as a successful graph representation, but more convenient numerically. Secondly, we adopt the nonlinear combination of the eigenvector elements, to make our invariant more general and informative. Finally, as pointed out for each PFO separately in the following, the proposed PFOs convey useful information about the graph structure and enrich our invariant.

Definition 2. *Power PFO:* The power PFO of graph G is a $N \times \Omega$ matrix named $\dot{G}$, whose column $\omega \in \mathcal{W} = \{\omega_1, \omega_2, \ldots, \omega_\Omega\}$ is the power PFO of order ω of G and computed as follows:

$$\dot{G}^{\omega} = [\textstyle\sum_{u=1}^{N} \phi_1(u)^{\omega}, \sum_{u=1}^{N} \phi_2(u)^{\omega}, \ldots, \sum_{u=1}^{N} \phi_N(u)^{\omega}]^T. \quad \square \tag{17}$$

The power PFO of order 0 is the number of graph vertices and is constant over the eigen-modes. Therefore, as it will be shown in Section 2.4, utilizing power PFO of order 0 in proposed GeFFE method, removes the effect of the eigenvector elements, so it makes possible for GeFFE to generate the effect of eigenvalue-dependent feature vectors such as the Laplacian spectrum. The power PFO of order 1 is the Fourier transform and it conveys the notion of frequency. The increasing powers emphasize higher-value components of the eigenvector like a kind of soft-max function. In terms of the graph structure, this emphasizes graphs where a single node has a strong response at a particular frequency, as $\sum_{u=1}^{N} \phi_1(u)^{\omega}$ will be large in this case. The transform functions are, however, not longer orthogonal.

Definition 3. *Correlated PFO:* The correlated PFO of graph G is a $N \times \Omega$ matrix named $\ddot{G}$, whose column $\omega \in \mathcal{W} = \{\omega_1, \omega_2, \ldots, \omega_\Omega\}$ is the correlated PFO of order ω and computed as follows:

$$\begin{aligned}\ddot{G}^{\omega} = [&\sum_{u_1=1}^{N}\sum_{u_2=1}^{N}\cdots\sum_{u_\omega=1}^{N}(\phi_1(u_1)\phi_1(u_2)\ldots\phi_1(u_\omega)),\\ &\sum_{u_1=1}^{N}\sum_{u_2=1}^{N}\cdots\sum_{u_\omega=1}^{N}(\phi_2(u_1)\phi_2(u_2)\ldots\phi_2(u_\omega)),\\ &\vdots\\ &\sum_{u_1=1}^{N}\sum_{u_2=1}^{N}\cdots\sum_{u_\omega=1}^{N}(\phi_N(u_1)\phi_N(u_2)\ldots\phi_N(u_\omega))]^T.\end{aligned} \tag{18}$$

The correlated PFO of the orders 0 and 1 are equivalent to the power PFO of the same orders. The order 2 is the first order which the information of the correlation between different entities of the eigenvector is appeared on. This PFO measures the statistical correlation between the eigenvector elements at different orders. This therefore gives a large value when the frequency response of a group of nodes is the same (i.e. they have the same relationship to the rest of the graph).

2.4 Generalized Frequency Filtering Embedding

The generalized frequency filtering embedding is defined as follows:

Definition 4. *Generalized Frequency Filtering Embedding (GeFFE):* Let $\mathcal{F} = \{F_1, F_2, \ldots, F_r\}$ be the filter bank and $\mathcal{W} = \{\omega_1, \omega_2, \ldots, \omega_\Omega\}$ be the order set of the PFO. The generalized frequency filtering embedding $\gamma_{\mathcal{F},\mathcal{W}}$ is defined as:

$$\begin{aligned}&\gamma_{\mathcal{F},\mathcal{W}} : \mathcal{G} \rightarrow \mathbb{R}^{\Omega\times m\times r}\\ &\gamma_{\mathcal{F},\mathcal{W}}(G) = [\mathbf{f}_1^{\omega_1}(G)^T, \mathbf{f}_1^{\omega_2}(G)^T, \ldots, \mathbf{f}_1^{\omega_\Omega}(G)^T,\\ &\qquad\qquad \mathbf{f}_2^{\omega_1}(G)^T, \mathbf{f}_2^{\omega_2}(G)^T, \ldots, \mathbf{f}_2^{\omega_\Omega}(G)^T,\\ &\qquad\qquad \vdots\\ &\qquad\qquad \mathbf{f}_r^{\omega_1}(G)^T, \mathbf{f}_r^{\omega_2}(G)^T, \ldots, \mathbf{f}_r^{\omega_\Omega}(G)^T,],\end{aligned} \tag{19}$$

where $\mathcal{G}$ is the graph domain, m is the number of selected eigen-modes, and $\mathbf{f}_k^{\omega}(G) = [F_k(\lambda_j)\check{G}^{\omega}(\lambda_j), j = 1, \ldots, m]$ is the response of order ω of graph G to the filter F_k. where $\check{G}$ can be one of $\dot{G}$ and $\ddot{G}$, for instance. □

In the above definition, $\mathcal{F}$ and $\mathcal{W}$ can be selected statically or trained for each application. The second approach is more effective, because as it is shown in Sections 3.3 and 3.4, the best combinations of filters and PFOs vary for varying graph structures. The training process is described in Section 3.5.

By definition 4, we propose GeFFE as a general framework, which can formulate some previously-introduced invariants as the special cases, by choosing the appropriate filter function and the appropriate Fourier transform of different orders. The definitions of PFO as well as two sets $\mathcal{F}$ and $\mathcal{W}$ for these invariants are tabulated in Table 1. As it is clarified, GeFFE can formulate both the spectrum-based invariants like Laplacian spectrum by removing the impact of the Fourier transform and the eigenvector-based invariants like symmetric polynomials by removing the impact of eigenvalues. GeFFE can generate more complicated invariants like eigen-modes and the heat content power series coefficients by getting both eigenvalues and eigenvectors involved in GeFFE vector computation. In the last case, the mth element of the embedded vector q is:

$$q_m = \sum_{k=1}^{N}\left((\sum_{u=1}^{N}\phi_k(u))^2\frac{(-\lambda_k)^m}{m!}\right). \tag{20}$$

The embedded vector of GeFFE is more informative, because it possesses the components themselves not their summation. For full equivalence, the applied classifier should be able to simulate the impact of summation for the vector components.

TABLE 1: The Previously Defined Invariants as the Special Case of GeFFE.

Invariant	$\mathcal{F}$	$\mathcal{W}$	$\check{G}^{\omega}$
Lspec	$\{\lambda_k \mid k = 1, 2, \ldots, N\}$	$\{0\}$	$\dot{G}^{\omega}$
Ftran	$\{1 \mid k = 1, 2, \ldots, N\}$	$\{1\}$	$\dot{G}^{\omega}$
Poly	$\{1 \mid k = 1, 2, \ldots, N\}$	$\{1, 2, \ldots, \lvert V\rvert\}$	$\ddot{G}^{\omega}$
Emod	$\{\lambda_k \mid k = 1, 2, \ldots, N\}$	$\{1\}$	$\dot{G}^{\omega}$
HIP	$\left\{\frac{(-\lambda_k)^1}{1!}, \frac{(-\lambda_k)^2}{2!}, \ldots, \frac{(-\lambda_k)^m}{m!} \mid k = 1, 2, \ldots, N\right\}$	$\{2\}$	$\left[(\sum_{u=1}^{N}\phi_k(u))^{\omega} \mid k = 1, 2, \ldots, N\right]^T$

Lspec, Ftran, Poly, Emod and HIP stand for Laplacian-spectra, Fourier transform, Symmetric polynomials [14], Eigen-mode [6] and Heat content power series coefficients [45], respectively.

3 Experimental Results

In this section, some experimental results are reported to show the effect of GeFFE in differentiating and classification of different graphs with different properties. All the classification accuracies are estimated using 5NN classifier and 5 fold cross validation and the average of 10 runs are reported. A set of diverse datasets collected from different related papers are used in the experiments of this paper. The graphs of mutag dataset [46] represent the chemical compounds which are classified to be mutagen or not. In PTC dataset [47] , the objective is to detect the carcinogenicity of the chemical compounds from their graphs. The graphs of Enzymes dataset [48] represent the tertiary structure of proteins in two types of enzymes. PPI [49] is the dataset of the protein-protein interaction networks in two types of bacteria. CATH2 [48] consists of the graphs of the proteins and the objective is to detect the homogeneity class. Protein dataset [50] is composed of the protein structure of six types of the enzymes. Shock dataset [51] is constructed from the skeletal structures of 2D objects. Llow, Lmed and Lhigh datasets [50] consist of the graphs of hand-writing letters with low, medium and high distortions, respectively. The objective is to detect the class (i.e. a, b, ...,z) of the input letter. COIL15 [50] and ODBK50 [52] are two object detection datasets composed of the object structural graphs whose vertices are extracted through corner detection and edges are inserted through triangulation. The properties of these datasets are tabulated in Table 2.

The proposed methods are compared with some previous graph embedding methods including: Laplacian Spectrum

TABLE 2: The Real Graph Datasets.

Dataset	#Vertices (min, max, ave)	#Edges (min, max, ave)	#Graphs	#Classes
mutag	(14, 40, 26.03)	(26, 84, 53.78)	188	2
PTC	(2, 109, 25.56)	(2, 216, 51.92)	344	2
Enzymes	(2, 126, 32.63)	(1, 149, 62.14)	600	2
PPI	(3, 232, 109.60)	(4, 3006, 864.37)	86	2
CATH2	(143, 568, 307.99)	(556, 2220, 1254.8)	190	2
Protein	(2, 126, 32.63)	(1, 149, 62.14)	600	6
Shock	(4, 33, 13.17)	(6, 64, 24.33)	150	10
Llow	(1, 8, 4.68)	(0, 6, 3.13)	2250	15
Lmed	(1, 9, 4.67)	(0, 7, 3.21)	2250	15
Lhigh	(1, 9, 4.67)	(0, 9, 4.5)	2250	15
COIL15	(18, 77, 42.73)	(45, 222, 116.49)	585	15
ODBK50	(41, 200, 123.23)	(106, 589, 352.81)	600	50

(Lspec), the symmetric polynomials signature (Poly) [14], the number of backtrackless walks of different lengths (BTW) [17], Ihara zeta functions (IZF) [16], heat kernel trace (HIT) and power series expansion coefficients of heat content (HIP) [45], the number of random walks of different lengths (RW) [12], the sorted elements of wave kernel (WK) [53], the histogram and sorted values of node HKSs (KShist and HKSsort) [44].

3.1 Following the edit distance

In an appropriate embedding method, the trend of changing in the feature distance should obey from the trend of changing in edit distance. It means that two graphs with small edit distance should have a small feature distance and vice versa. This behavior is studied in this experiment. For this purpose, four random graphs are produced through four different methods as the seed graphs. The first one is a Delaunay triangulation graph with 100 nodes whose (x, y) coordinates are real numbers picked from [1,100] randomly. The second seed graph is an erdős-Rényi model with 100 nodes and 130 edges. The third seed graph is a geometric graph with 100 nodes whose 3-dimension coordinates are picked randomly from [0,1] and two nodes are connected if they are in 0.5 radius neighborhood of each other. The last random graph is a small world graph with average degree 6 and random rewiring probability 0.2. The seed graphs are shown in the column a of the Fig. 2. In separate tests, 30 variations of every seed graph are made by random consecutive edge deletions. This process is repeated 1000 times and yields the set of 1000 graphs for every edit distance 1 to 30 from the seed graph. The column b of Fig. 2 shows the mean FFE feature distance against the edit distance for every corresponding seed graph. The filter set is $\mathcal{F} = \{X\} \cup \{PS_{r,11} | 1 \leq r \leq 11\}$ and the 12 filter responses are inserted in a long vector. As it is observed, FFE cannot differentiate between edited graphs. The reason is that the positive and negative eigenvector elements cancel each other and produce the small values as the elements of Fourier transform for all graphs. The columns c and d of the Fig. 2 correspond to the long vectors of GeFFE using the mentioned filter set and the orders $\mathcal{W} = \{0, 1, 4\}$ of $\dot{G}$ and $\ddot{G}$, respectively. The resulting vectors have the meaningful feature distances with each other, however the feature distances of GeFFE by $\dot{G}$ exhibit less standard deviation in average and its change is more monotonic.

3.2 Cospectrality

The purpose of this experiment is to study the power of the proposed embedding methods to differentiate cospectral graphs. For this experiment, three groups of the strongly regular graphs (SRGs) and 2 groups of Balanced Incomplete Block Designs (BIBDs) are used. $SRG(v, k, \lambda, \mu)$ is a k-regular v-node graph which every pair of its adjacent nodes has λ common neighbors and every pair of its non-adjacent nodes has μ common neighbors. $BIBD(v, k, \lambda)$ is a v-node graph consisting of k-node blocks such that every pair of the graph nodes is placed in λ blocks. The graphs of every group has the identical parameters and the identical Laplacian spectrum, however they are not isomorphic. FFE by the identity filter (FFE), GeFFE by the identity filter and $\dot{G}$ of order 4 (GeFFE1), and GeFFE by the identity filter and $\ddot{G}$ of order 4 (GeFFE2) are compared with each other and with previous methods in cospectrality reduction. The point should be noted is that since just one filter and one Fourier order is selected, the embedded vector length is N for all three proposed methods. The results are tabulated in Table 3. It can be seen that FFE can not differentiate the tested cospectral graphs, while both GeFFE1 and GeFFE2 are able to obtain the best possible result in this experiment. The Poly method could obtain this result, but the length of its feature vector is N^2. IZF method is another method which could obtain the similar result, but in $O(N^6)$ time in comparison with $O(N^3)$ of GeFFE1 and $O(N^5)$ of GeFFE2.

TABLE 3: The Amount of Cospectrality in Proposed Methods.

group	SRG $(25, 12, 5, 6)$	SRG $(26, 10, 3, 4)$	SRG $(36, 15, 6, 6)$	$BIBD$ $(15, 3, 1)$	$BIBD$ $(23, 11, 5)$
Lspec	105	45	25651	946	611065
Poly	0	0	0	0	0
BTW	105	45	25651	946	611065
IZF	0	0	0	0	0
HIT	105	45	25651	946	611065
HIP	105	45	25651	946	611065
RW	105	45	25651	946	611065
WK	105	45	25651	946	611065
HKSsort	105	45	25651	946	611065
HKShist	105	45	25651	946	611065
FFE	105	45	25651	946	611065
GeFFE1	0	0	0	0	0
GeFFE2	0	0	0	0	0
#gp	105	45	25651	946	611065

The tabulated numbers are the number of cospectral graph pairs.
#gp stands for the total number of graph pairs in the group.

3.3 The comparison between different filters

The purpose of this experiment is to show that different filters reveal different structural properties of graphs. So using different filter responses is beneficial. We reason about our claim in this experiment by showing that GeFFE vectors of some different filters obtain different classification accuracies in real datasets with different characteristics.

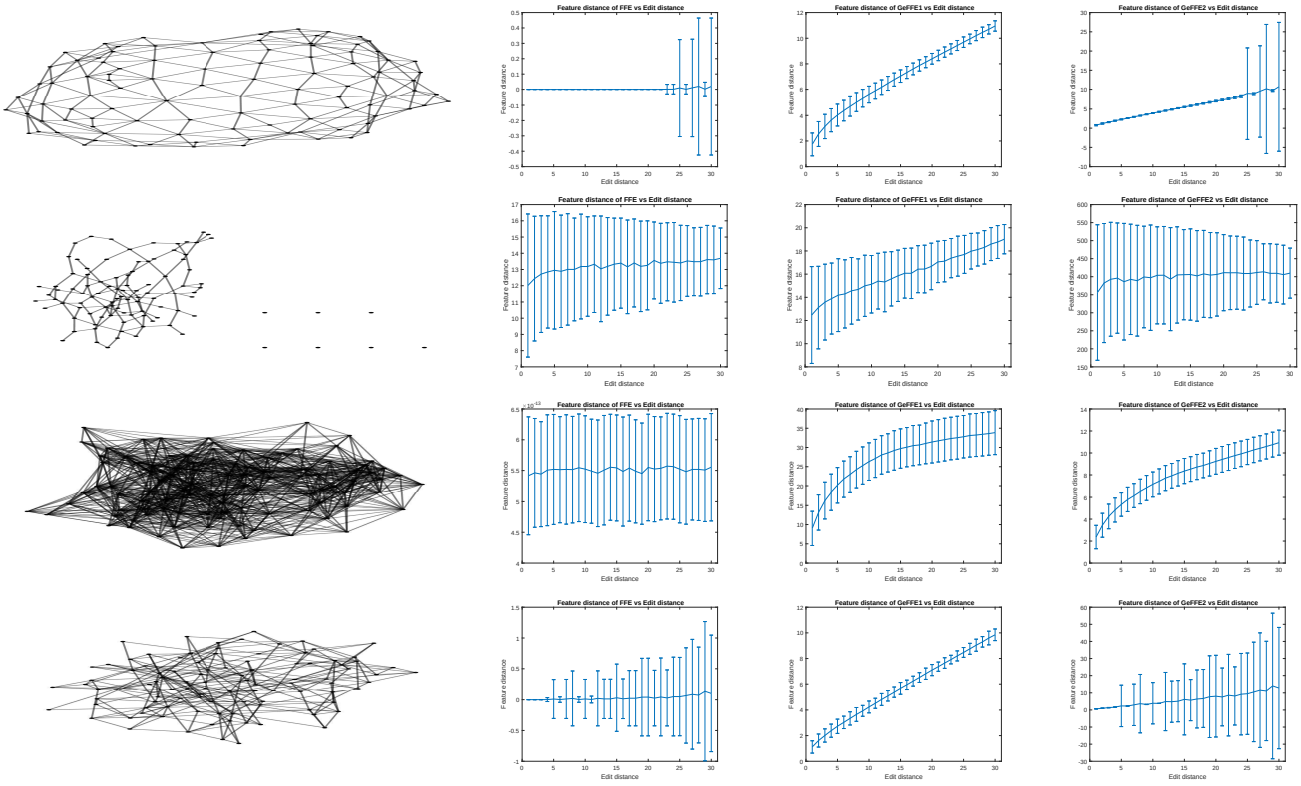

Fig. 2: The feature distances of different proposed methods in comparison with the edit distance. Column a: Seed graphs. Column b: FFE method. Column c: GeFFE by power PFO. Column d: GeFFE by correlated PFO.

Fig. 3 plots the classification accuracies of embedded vectors of GeFFE by order 4 of $\dot{G}$ and each time by one of the filters of the set $\{X, H_1, H_3, H_6, AH_1, AH_3, AH_6, PS_{1,11}, PS_{6,11}, PS_{11,11}\}$ for all tested datasets. It can be seen that different filters have different effects in classification of the different datasets. We can see that the heat filters perform much better than the anti-heat on CATH2, which can be explained by the fact that the task is to find the homogeneity class which is related to large-scale structure. On the other hand, anti-heat performs better on PPI, suggesting the detailed connectivity is more important in this dataset. On the others, information is contained over the whole spectrum. The part-sine filter emphasizes narrow bands, which allows us to see where the important structure is localized to one particular scale.

The notable point is that although the heat filters are known as the informative filters in different researches (but in other areas), these filters are not the best filters in all cases. Fig. 4 compares the classification accuracies of the long vectors of three different filter combinations XHAP, XAP and XP with each other. $\mathcal{F}_{XHAP} = \{X\} \cup \{H_t | 1 \leq t \leq 6\} \cup \{AH_t | 1 \leq t \leq 6\} \cup \{PS_{r,11} | 1 \leq r \leq 11\}$, $\mathcal{F}_{XAP} = \{X\} \cup \{AH_t | 1 \leq t \leq 6\} \cup \{PS_{r,11} | 1 \leq r \leq 11\}$, and $\mathcal{F}_{XP} = \{X\} \cup \{PS_{r,11} | 1 \leq r \leq 11\}$. It can be seen that the filter combination including heat filters has the lower classification accuracies in all the cases. The small scale between-node interactions, whose effect appear on high frequencies, play important role in differentiating the graphs of the applications. When heat filters attenuate the high frequencies to decrease the effect of the noise, this beneficial information is lost as well. This behavior is shown in Fig. 5. The similar tests of Section 3.1 is performed using the long vectors constructed by orders {0,1,4} of $\dot{G}$ and each time by one of the proposed filter functions. Edges are considered as representatives for small scale substructures and removing them is studied. The heat filter functions and $PS_{1,11}$ filter function are worst in following edit distance. The feature distances change very slowly and this change is not monotonic. This behavior is observed because these filters alleviate the effect of changing the small scale structures in feature distance. This effect is beneficial in noise reduction, where the value of these small scale substructures in differentiating the graphs is negligible; however it is not true for the applications in hand. Furthermore, although the heat kernel is known as a good solution for the problem of noise sensitivity in eigen-modes by down-weighting the high frequencies [42], but this belief is not necessarily true in all the applications. The stability of eigen-modes is dependent on the spectral gap (gap between consecutive eigenvalues) and depends on the graph structure as well as the frequency. Where noise and irrelevant local structural errors occur, this would affect the high-frequency components adversely, but this is not true of all graph data. Our experiments show this.

Another point is that the datasets with similar structures have the similar reactions to different filters. This phenomenon can be seen more precisely in Fig. 6(a) to (f) for different Fourier orders in 3 datasets Llow, Lmed and Lhigh as the similar set 1 and in Fig. 6(g) to (l) for two datasets

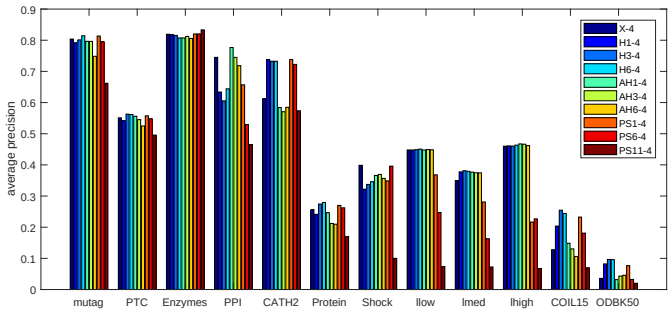

Fig. 3: The classification accuracies of GeFFE by some different filters and order 4 of $\dot{G}$.

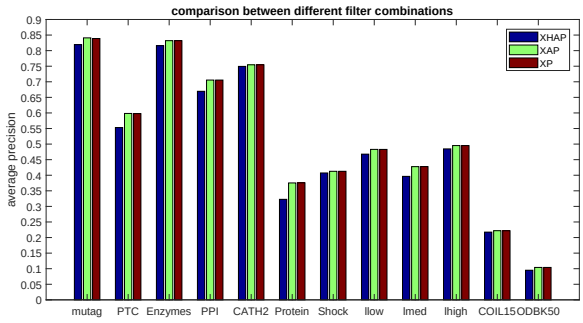

Fig. 4: The classification accuracies of some different filter combinations using three selected combination strategies.

COIL15 and ODBK50 as the similar set 2. It suggests an acceptable relation between the frequency filtering operator and graph structure and makes the hope that the GeFFE strategy is effective enough to extract the similar structures in different datasets, however the approval of this claim needs more investigation.

3.4 The comparison between different PFO orders

The experiment similar to the experiment of the previous section is done for different PFO orders to show the benefits of using them. The GeFFE vectors of $PS_{4,11}$ filter, each time with one of the orders of the set $\{0, 1, 2, 3, 4, 5\}$ of $\dot{G}$ are used in this experiment and the accuracies is plotted in Fig. 7 for all tested datasets. The similar effect of the previous sub-section is observable for different orders. The effectiveness of a special order differs from a dataset to another. For example, the order 0 has the highest importance in mutag, PPI and CATH2 and the lowest importance in PTC and lhigh. The similar effect can be observed in order 4 which is the most important order in Enzymes, Shock, llow, lmed and lhigh datasets, while it has the third rank in PTC, Protein, COIL15 and ODBK50. The ability of discovering similar structures can be seen more and less in this experiment, too. This results and the results of the previous sub-section suggest that different combinations of the filters and the Fourier orders include useful information and the appropriate combination of them should be applied based on the application in hand. Different datasets have different properties, and machine learning can use these features to learn the most appropriate representation.

3.5 GeFFE vs other embedding methods

The main purpose of embedding methods is to map the similar graphs into close vectors and the dissimilar graphs into far ones. The experiment reported in Section 3.1 showed that GeFFE vectors exhibited this property in a synthetic graph set. The purpose of this experiment is to evaluate GeFFE for having the mentioned property in real graphs. Classification using the simple classifier 5NN can help us to estimate the amount of this property.

GeFFE by the filter set $\mathcal{F} = \{X\} \cup \{H_t | 1 \leq t \leq 6\} \cup \{AH_t | 1 \leq t \leq 6\} \cup \{PS_{r,11} | 1 \leq r \leq 11\}$ and the order set $\mathcal{W} = \{0, 1, 4\}$ of $\dot{G}$ is compared with the other embedding methods in Table 5. In the first version of the method, *GeFFE-all*, the long vector of all filter responses is considered as the feature vector. *GeFFE-all* obtained the average rank 2.58 among 11 tested methods, which makes it comparable with the other methods. However, *GeFFE-all* can not reach the best accuracy in all tested datasets. The reason is that as it is shown in Section 3.3 and Section 3.4, different filters and different orders have different importance in different datasets, but in *GeFFE-all*, all of the filter responses are inserted into the feature vector and participate in the clustering process with the same importance, regardless of the properties of the underlying dataset. Consequently, for taking full advantage of the information revealed by the filter responses, it is necessary to learn the importance degree of each filter response and use this degree in the clustering process.

We followed this aim by applying forward selection on filter responses. The graph response to the specific filter and the specific order of PFO is considered as a feature group, yielding $r \times \Omega$ feature groups. The forward selection starts with an empty feature set and at each step, the feature group which better enhances the classification accuracy in training data is added to the selected feature groups. 10 first selected feature groups for the tested datasets are tabulated in Table 4. According to these results, 4 versions of GeFFE are applied to the datasets and the results are reported in Table 5. The feature vectors of *GeFFE-best-filter* and *GeFFE-best-5-filters* are composed of the first and 5 first selected feature groups in forward selection process, respectively. In *GeFFE-local-max*, the selected feature groups are used until the step where its 10 future steps could not enhance the accuracy. In *GeFFE-global-max*, the feature groups are used until the step where the max accuracy in training data is obtained. The average number of filter responses in *GeFFE-local-max* and *GeFFE-global-max* over tested datasets are 7.08 and 17.08, respectively. As it can be seen, *GeFFE-global-max* is the best performing method. However the other 3 versions of GeFFE outperforms the previous methods in all the tested datasets (except a case of GeFFE-best-filter where the difference is negligible). The first point that can be perceived from the results is that the selected filters and PFOs are efficient enough for our purpose and the second point is that our strategy in selecting suitable filter responses for the datasets could adopt GeFFE to the structural properties of different datasets.

It should be noted that in *GeFFE-best-filter* the feature vector length is N, which is less or equal to the vector lengths of the other methods. Generally, the feature vector length of

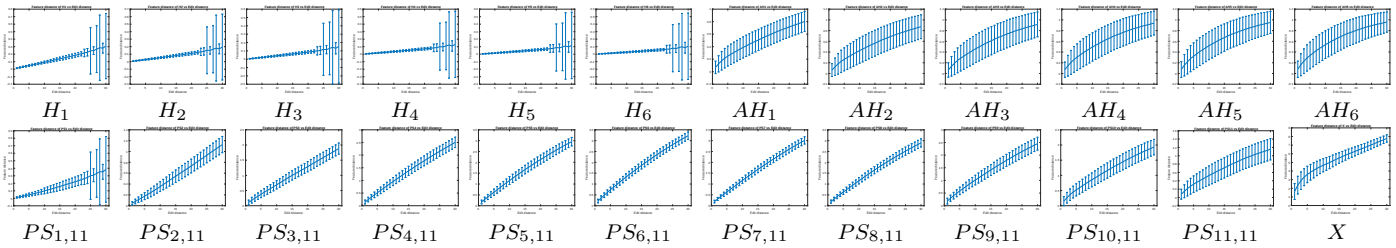

Fig. 5: The test of following edit distance for proposed filter functions.

TABLE 4: The 10 First Selected Filter Responses Using Forward Selection on the GeFFE Filter Responses.

	mutag	PTC	Enzymes	PPI	CATH2	Protein	Shock	Llow	Lmed	Lhigh	COIL15	ODBK50
1	AH_5-0	X-1	PS_{11}-0	AH_4-0	AH_3-0	AH_2-0	AH_6-0	PS_{11}-0	PS_{11}-0	PS_{11}-0	AH_4-0	AH_1-0
2	AH_6-0	AH_2-1	AH_6-0	AH_6-0	AH_2-0	AH_3-0	AH_5-0	AH_6-1	AH_4-1	AH_6-1	AH_3-0	AH_2-0
3	X-1	AH_3-1	AH_4-0	AH_3-0	AH_5-0	X-0	AH_3-0	AH_2-1	AH_5-1	AH_5-1	AH_5-0	AH_3-0
4	AH_4-0	AH_6-1	AH_3-0	AH_5-0	AH_4-0	AH_4-0	AH_4-0	AH_3-1	AH_3-1	AH_4-1	X-1	AH_4-0
5	AH_3-0	AH_4-1	AH_5-0	AH_2-0	AH_1-0	AH_5-0	AH_2-0	AH_4-1	AH_6-1	PS_{11}-1	AH_6-0	AH_5-0
6	AH_2-1	AH_5-1	AH_2-0	PS_{10}-0	AH_6-0	AH_1-0	AH_1-0	AH_5-1	AH_2-1	PS_{10}-1	AH_2-0	AH_6-0
7	AH_3-1	AH_1-1	AH_4-1	PS_9-0	X-1	AH_6-0	PS_{11}-0	AH_1-1	PS_{11}-1	AH_3-1	PS_{11}-0	X-1
8	AH_1-1	AH_6-0	X-1	PS_7-0	PS_{11}-0	PS_{11}-0	AH_3-1	PS_6-1	AH_1-1	PS_{11}-4	AH_1-1	AH_1-1
9	AH_2-0	PS_2-1	AH_2-1	PS_8-0	AH_1-1	X-1	AH_2-1	H_2-0	PS_{10}-1	PS_{10}-0	AH_2-1	PS_{11}-0
10	AH_4-1	PS_4-1	AH_3-1	PS_{11}-0	AH_2-1	AH_1-1	AH_4-1	H_1-0	PS_6-1	AH_2-1	AH_3-1	AH_2-1

$PS_{i,11}$ is briefly indicated by PS_i.

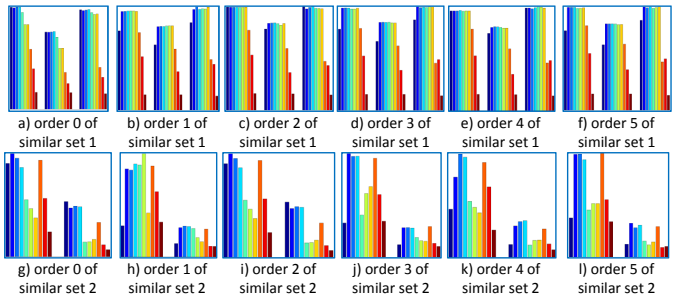

Fig. 6: The similar reactions of different filters on the structurally similar datasets. The similar set 1 is {Llow, Lmed and Lhigh} and the similar set 2 is {COIL15 and ODBK50}.

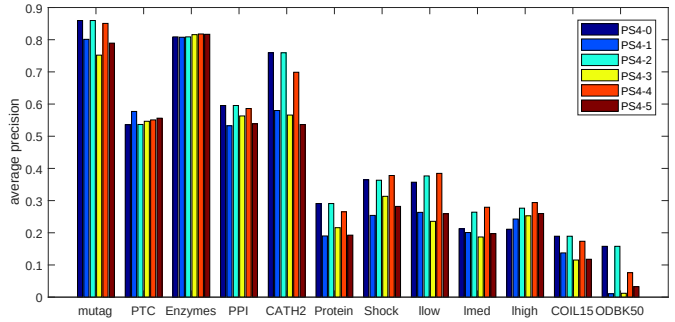

Fig. 7: The classification accuracies of GeFFE by $PS_{4,11}$ filter and different orders of $\dot{G}$.

GeFFE method using power PFOs is of $O(N)$ and its time complexity is of $O(N^3)$ just like the majority of the other spectral methods. Of course, its training time depends on the used feature selection strategy.

4 Conclusion

In this article, a novel embedding method named GeFFE is proposed using the graph signal processing operators: frequency filtering and Fourier transform. Frequency filtering amplifies or attenuates the contribution of different eigenvalues and the proposed pseudo-Fourier operators expands graph Fourier transform to make diverse invariant combinations of eigenvector elements. The conclusion remarks of this article can be listed as follows:

1) GeFFE benefits from the information of both eigenvalues and eigenvectors, hence it has the ability of discovering:
   (a) Structural similarities. GeFFE (especially by power PFOs) can simulate the edit distance in random variations of a seed graph.
   (b) Structural differences: GeFFE by both power and correlated PFOs can differentiate some groups of Laplacian cospectral graphs from each other entirely.
2) GeFFE has the ability to concentrate on a special portion of the spectrum and explore its latent structural information. In this regard:
   (a) Some filter functions were proposed. It was experimentally shown that some filter sets excluding the heat filters results in better classification accuracies. This observation opens the possibility of discovering more powerful filter functions.
   (b) Different filter functions are different in graph classification. So training their importance in the application in hand is beneficial.
   (c) The same filter function shows the same relative classification accuracies in structurally similar datasets. This effect can be observed more and less in different orders of a filter. This phenomenon introduces GeFFE as a candidate for discovering the sub-structures in

TABLE 5: The Classification Accuracies of Some Versions of GeFFE in Comparison With the Existing Embedding Methods.

	mutag	PTC	Enzymes	PPI	CATH2	Protein	Shock	Llow	Lmed	Lhigh	COIL15	ODBK50
Lspec	83.32	59.96	82.28	70.57	75.59	38.07	40.73	44.76	34.41	44.36	26.35	15.59
Poly	77.51	52.24	80.98	60.94	07.37	29.22	40.00	37.36	32.48	48.84	16.63	2.36
BTW	83.57	53.67	81.05	66.37	72.48	26.02	35.33	32.12	24.81	27.02	27.36	14.74
IZF	81.43	44.16	81.72	46.54	57.37	16.93	10.00	6.67	6.73	17.87	6.79	2.00
HIT	56.54	49.82	82.58	43.67	53.42	16.93	7.40	12.38	11.74	10.68	7.61	1.57
HIP	56.07	51.32	81.08	48.33	41.31	22.08	16.27	13.08	13.36	10.77	7.60	1.52
RW	81.12	54.01	81.46	64.84	71.84	21.08	35.20	35.73	29.39	29.83	19.06	0.37
WK	78.87	54.64	81.04	62.57	72.11	22.92	37.40	45.00	40.90	37.02	18.64	8.08
HKSsort	78.88	55.09	79.52	71.61	74.48	25.48	38.47	43.87	35.71	44.48	22.98	12.94
HKShist	63.87	45.38	82.17	57.10	54.76	18.05	8.80	6.78	6.67	6.72	5.80	1.22
GeFFE-all	81.92	55.30	81.58	66.95	74.94	32.27	40.73	**46.77**	39.64	48.46	21.75	9.51
GeFFE-best-filter	**89.90**	**66.04**	**84.93**	**84.16**	**80.89**	**37.40**	**49.40**	**47.03**	40.50	**49.66**	**31.22**	**17.78**
GeFFE-best-5-filters	**90.38**	**68.82**	**85.73**	**86.24**	**83.10**	**42.57**	**55.47**	**47.45**	**41.13**	**51.35**	**33.72**	**20.98**
GeFFE-local-max	**90.86**	**69.44**	**85.92**	**86.83**	**83.73**	**42.75**	**56.13**	**47.46**	**41.25**	**51.87**	**33.99**	**21.25**
GeFFE-global-max	**91.07***	**71.53***	**86.43***	**87.89***	**84.73***	**44.05***	**57.13***	**47.48***	**41.34***	**52.23***	**34.82***	**21.68***

The best accuracies for each dataset is determined by the * symbol.
The accuracies of GeFFE versions which are better than all the accuracies of the other previous methods are indicated with bold face.

different datasets.

3) Training the best performing filter responses through forward selection is a good strategy for adopting GeFFE to the structural properties of different datasets. Through this strategy, GeFFE even using just the best filter response has the superior performances against existing embedding methods in classification the tested datasets.
4) GeFFE can play the role of the general framework to formulate some graph invariants which make use of eigenvalues, eigenvectors or both of them.
5) GeFFE has the potential to be more efficient by defining other filters in order to explore the spectrum more precisely and other PFOs in order to combine the eigenvector elements in different ways.

For further assessment on this new trend, we plan to explore the new filter functions as well as the new methods for composing PFOs. Some specially-designed synthetic datasets can be helpful for designing a useful filter-bank which each of its members is appropriate for discovering a special graph substructure. A similar investigation should be done for discovering the detailed relation between different PFOs and PFO orders with graph structures. A method is needed to discover more informative portions of the spectrum for each dataset and analyze this portion more precisely. Spectral invariants usually consider only unlabeled or sometimes labeled graphs, but not attributes. Using graph signal gives GeFFE the potential of handling attributed graphs, however this potential ability should be investigated in detail.

REFERENCES

[1] C. M. Bishop, *Pattern recognition and machine learning*. Springer, 2006.
[2] K. Fukunaga, *Introduction to statistical pattern recognition*. Academic press, 2013.
[3] M. Alvarez Vega, "Graph kernels and applications in bioinformatics," Ph.D. dissertation, Utah State University, 2011.
[4] H. Bunke and K. Riesen, "Recent advances in graph-based pattern recognition with applications in document analysis," *Pattern Recognition*, vol. 44, no. 5, pp. 1057–1067, 2011.
[5] H.-P. Kriegel, P. Kröger, M. Renz, and T. Schmidt, "Hierarchical graph embedding for efficient query processing in very large traffic networks," in *International Conference on Scientific and Statistical Database Management*. Springer, 2008, pp. 150–167.
[6] B. Luo, R. C. Wilson, and E. R. Hancock, "Spectral embedding of graphs," *Pattern recognition*, vol. 36, no. 10, pp. 2213–2230, 2003.
[7] S. Günter and H. Bunke, "Self-organizing map for clustering in the graph domain," *Pattern Recognition Letters*, vol. 23, no. 4, pp. 405–417, 2002.
[8] H. Bunke and K. Riesen, "Towards the unification of structural and statistical pattern recognition," *Pattern Recognition Letters*, vol. 33, no. 7, pp. 811–825, 2012.
[9] J. Gibert, E. Valveny, and H. Bunke, "Graph embedding in vector spaces by node attribute statistics," *Pattern Recognition*, vol. 45, no. 9, pp. 3072–3083, 2012.
[10] D. Haussler, "Convolution kernels on discrete structures," Citeseer, Tech. Rep., 1999.
[11] R. I. Kondor and J. Lafferty, "Diffusion kernels on graphs and other discrete input spaces," in *ICML*, vol. 2, 2002, pp. 315–322.
[12] T. Gärtner, P. Flach, and S. Wrobel, "On graph kernels: Hardness results and efficient alternatives," in *Learning Theory and Kernel Machines*. Springer, 2003, pp. 129–143.
[13] H. Bunke, S. Günter, and X. Jiang, "Towards bridging the gap between statistical and structural pattern recognition: Two new concepts in graph matching," in *International Conference on Advances in Pattern Recognition*. Springer, 2001, pp. 1–11.
[14] R. C. Wilson, E. R. Hancock, and B. Luo, "Pattern vectors from algebraic graph theory," *IEEE Transactions on Pattern Analysis and Machine Intelligence*, vol. 27, no. 7, pp. 1112–1124, 2005.
[15] P. Ren, R. C. Wilson, and E. R. Hancock, "Spectral embedding of feature hypergraphs," in *Joint IAPR International Workshops on Statistical Techniques in Pattern Recognition (SPR) and Structural and Syntactic Pattern Recognition (SSPR)*. Springer, 2008, pp. 308–317.
[16] ——, "Graph characterization via ihara coefficients," *IEEE Transactions on Neural Networks*, vol. 22, no. 2, pp. 233–245, 2011.
[17] F. Aziz, R. C. Wilson, and E. R. Hancock, "Backtrackless walks on a graph," *IEEE transactions on neural networks and learning systems*, vol. 24, no. 6, pp. 977–989, 2013.
[18] B. Xiao, "Heat kernel analysis on graphs," Ph.D. dissertation, The University of York, 2007. 2, 2007.
[19] H. Bahonar, A. Mirzaei, and R. C. Wilson, "Diffusion wavelet embedding: A multi-resolution approach for graph embedding in vector space," *Pattern Recognition*, vol. 74, pp. 518–530, 2018.
[20] B. Bonev, F. Escolano, D. Giorgi, and S. Biasotti, "Information-theoretic selection of high-dimensional spectral features for structural recognition," *Computer Vision and Image Understanding*, vol. 117, no. 3, pp. 214–228, 2013.
[21] R. N. Bracewell and R. N. Bracewell, *The Fourier transform and its applications*. McGraw-Hill New York, 1986, vol. 31999.
[22] J. S. Lim, "Two-dimensional signal and image processing," *Englewood Cliffs, NJ, Prentice Hall, 1990, 710 p.*, 1990.

[23] J. Brault and O. White, "The analysis and restoration of astronomical data via the fast fourier transform," *Astronomy and Astrophysics*, vol. 13, p. 169, 1971.
[24] J. R. Ferraro and L. J. Basile, *Fourier Transform Infrared Spectra: Applications to Chemical Systems*. Academic press, 2012.
[25] D. I. Shuman, S. K. Narang, P. Frossard, A. Ortega, and P. Vandergheynst, "The emerging field of signal processing on graphs: Extending high-dimensional data analysis to networks and other irregular domains," *IEEE Signal Processing Magazine*, vol. 30, no. 3, pp. 83–98, 2013.
[26] F. Zhang and E. R. Hancock, "Graph spectral image smoothing using the heat kernel," *Pattern Recognition*, vol. 41, no. 11, pp. 3328–3342, 2008.
[27] D. K. Hammond, P. Vandergheynst, and R. Gribonval, "Wavelets on graphs via spectral graph theory," *Applied and Computational Harmonic Analysis*, vol. 30, no. 2, pp. 129–150, 2011.
[28] W.-S. Kim, S. K. Narang, and A. Ortega, "Graph based transforms for depth video coding," in *2012 IEEE International Conference on Acoustics, Speech and Signal Processing (ICASSP)*. IEEE, 2012, pp. 813–816.
[29] M. Crovella and E. Kolaczyk, "Graph wavelets for spatial traffic analysis," in *INFOCOM 2003. Twenty-Second Annual Joint Conference of the IEEE Computer and Communications. IEEE Societies*, vol. 3. IEEE, 2003, pp. 1848–1857.
[30] N. Sidere, P. Héroux, and J.-Y. Ramel, "A vectorial representation for the indexation of structural informations," *Structural, Syntactic, and Statistical Pattern Recognition*, pp. 45–54, 2008.
[31] M. M. Luqman, J.-Y. Ramel, J. Lladós, and T. Brouard, "Fuzzy multilevel graph embedding," *Pattern Recognition*, vol. 46, no. 2, pp. 551–565, 2013.
[32] J. Gibert, E. Valveny, and H. Bunke, "Feature selection on node statistics based embedding of graphs," *Pattern Recognition Letters*, vol. 33, no. 15, pp. 1980–1990, 2012.
[33] E. Pekalska and R. P. Duin, "Classifiers for dissimilarity-based pattern recognition," in *Pattern Recognition, 2000. Proceedings. 15th International Conference on*, vol. 2. IEEE, 2000, pp. 12–16.
[34] K. Riesen and H. Bunke, "Graph classification based on vector space embedding," *International Journal of Pattern Recognition and Artificial Intelligence*, vol. 23, no. 06, pp. 1053–1081, 2009.
[35] E. Z. Borzeshi, M. Piccardi, K. Riesen, and H. Bunke, "Discriminative prototype selection methods for graph embedding," *Pattern Recognition*, vol. 46, no. 6, pp. 1648–1657, 2013.
[36] A. Fischer, K. Riesen, and H. Bunke, "An experimental study of graph classification using prototype selection," in *Pattern Recognition, 2008. ICPR 2008. 19th International Conference on*. IEEE, 2008, pp. 1–4.
[37] R. P. Duin and E. Pekalska, "The dissimilarity space: Bridging structural and statistical pattern recognition," *Pattern Recognition Letters*, vol. 33, no. 7, pp. 826–832, 2012.
[38] K. Riesen and H. Bunke, "Classifier ensembles for vector space embedding of graphs," in *International Workshop on Multiple Classifier Systems*. Springer, 2007, pp. 220–230.
[39] ——, "Approximate graph edit distance computation by means of bipartite graph matching," *Image and Vision computing*, vol. 27, no. 7, pp. 950–959, 2009.
[40] F. R. Chung, *Spectral graph theory*. American Mathematical Soc., 1997, vol. 92.
[41] H. El-Ghawalby and E. R. Hancock, "Geometric characterizations of graphs using heat kernel embeddings," in *IMA International Conference on Mathematics of Surfaces*. Springer, 2009, pp. 124–142.
[42] J. Sun, M. Ovsjanikov, and L. Guibas, "A concise and provably informative multi-scale signature based on heat diffusion," *Computer graphics forum*, vol. 28, no. 5, pp. 1383–1392, 2009.
[43] B. Xiao, E. R. Hancock, and R. C. Wilson, "Geometric characterization and clustering of graphs using heat kernel embeddings," *Image and Vision Computing*, vol. 28, no. 6, pp. 1003–1021, 2010.
[44] R. C. Wilson, "Graph signatures for evaluating network models," in *Pattern Recognition (ICPR), 2014 22nd International Conference on*. IEEE, 2014, pp. 100–105.
[45] B. Xiao, E. R. Hancock, and R. C. Wilson, "Graph characteristics from the heat kernel trace," *Pattern Recognition*, vol. 42, no. 11, pp. 2589–2606, 2009.
[46] A. K. Debnath, R. L. Lopez de Compadre, G. Debnath, A. J. Shusterman, and C. Hansch, "Structure-activity relationship of mutagenic aromatic and heteroaromatic nitro compounds. correlation with molecular orbital energies and hydrophobicity," *Journal of medicinal chemistry*, vol. 34, no. 2, pp. 786–797, 1991.
[47] G. Li, M. Semerci, B. Yener, and M. J. Zaki, "Effective graph classification based on topological and label attributes," *Statistical Analysis and Data Mining*, vol. 5, no. 4, pp. 265–283, 2012.
[48] L. Bai and E. R. Hancock, "Depth-based complexity traces of graphs," *Pattern Recognition*, vol. 47, no. 3, pp. 1172–1186, 2014.
[49] F. Escolano, E. R. Hancock, and M. A. Lozano, "Heat diffusion: Thermodynamic depth complexity of networks," *Physical Review E*, vol. 85, no. 3, p. 036206, 2012.
[50] K. Riesen and H. Bunke, "Iam graph database repository for graph based pattern recognition and machine learning," in *Joint IAPR International Workshops on Statistical Techniques in Pattern Recognition (SPR) and Structural and Syntactic Pattern Recognition (SSPR)*. Springer, 2008, pp. 287–297.
[51] L. Bai, L. Rossi, A. Torsello, and E. R. Hancock, "A quantum jensen–shannon graph kernel for unattributed graphs," *Pattern Recognition*, vol. 48, no. 2, pp. 344–355, 2015.
[52] S. F. Mousavi, M. Safayani, A. Mirzaei, and H. Bahonar, "Hierarchical graph embedding in vector space by graph pyramid," *Pattern Recognition*, vol. 61, pp. 245–254, 2017.
[53] M. Aubry, U. Schlickewei, and D. Cremers, "The wave kernel signature: A quantum mechanical approach to shape analysis," in *Computer Vision Workshops (ICCV Workshops), 2011 IEEE International Conference on*. IEEE, 2011, pp. 1626–1633.

Hoda Bahonar received her B.Sc and M.Sc. in computer engineering from Payam noor University and Tarbiat Modares Unviersity, in 2005 and 2009 respectively. She is currently pursuing her Ph.D. in Computer Engineering at Isfahan University of Technology, Isfahan, Iran. Her current research interests include Statistical and Structural Pattern Recognition and Graph clustering and classification.

Abdolreza Mirzaei received the B.Sc., M.Sc. and Ph.D. degrees in 2001, 2003, and 2009, respectively, from Isfahan University, Iran University of Science and Technology, and Amirkabir University of Technology. He is currently an assistant professor in the electrical and computer engineering department at Isfahan University of Technology, Iran. His research areas include Pattern Recognition, Machine Learning, Data Mining, and Swarm Intelligence.

Saeed Sadri received the B.S. and M.S. degrees in electrical engineering from the University of Tehran, Tehran, Iran, in 1977 and the Ph.D. degree from Isfahan University of Technology (IUT), Isfahan, Iran. Since 1980, he has been with the Department of Electrical and Computer Engineering, IUT. His research interests include signal and image processing, particularly image segmentation, with applications both in industry and medical science. He is a member of the DSP Laboratory, IUT, where he is engaged in computer vision, image processing, and data analysis.

Richard C. Wilson received the B.A. degree in physics from the University of Oxford, Oxford, U.K. in 1992, and the D.Phil. degree from the University of York, York, U.K. in 1996. He is currently a Professor with the Department of Computer Science, University of York. He has authored more than 200 papers in journals, edited books, and refereed conferences. His research interests include structural pattern recognition, graph methods for computer vision and novel imaging systems. He is a fellow of the IAPR and a senior member of IEEE.